Stabilization of the photorefractive double phase-conjugate mirror in $BaTiO_3$

C. Mailhan
Supélec, 2 rue Edouard Belin, 57070 Metz, France

N. Fressengeas
Laboratoire Matériaux Optiques, Photonique et Systèmes, Unité Commune à l'Université de Metz et à Supélec, CNRS-FRE 2304, 2 rue Edouard Belin, 57070 Metz, France

M. Goetz
Région Alsace, Direction de la Recherche, de l'Enseignement Supérieur et du Transfert de Technologies, Strasbourg, France

G. Kugel
Laboratoire Matériaux Optiques, Photonique et Systèmes, Unité Commune à l'Université de Metz et à Supélec, CNRS-FRE 2304, 2 rue Edouard Belin, 57070 Metz, France

(Received 27 June 2002; published 28 February 2003)

Photorefractive simple and double phase-conjugate mirrors very often exhibit strong instabilities in their reflectivities. One of their possible origins can be the competition between phase conjugation and its generating process, photorefractive beam fanning. However, by suitably choosing the incident beam widths and directions, we suppressed this competition and replaced it by the enhancement of each process by the other. This technique allows to obtain a double phase-conjugate mirror in $BaTiO_3$ that establishes itself in seconds for beam intensities on the order of the tenth of a milliwatt. The reflectivities reached are on the order of 30% and stable within 3% for hours.

DOI: 10.1103/PhysRevA.67.023817 PACS number(s): 42.65.Hw, 42.70.Nq

I. INTRODUCTION

The photorefractive double phase-conjugate mirror (DPCM) allows the obtention of two conjugated waves issued from two incoming extraordinary polarized beams: while the beam wave fronts are conjugated, their energy is exchanged. First demonstrated in $BaTiO_3$ by Weiss *et al.* [1] in 1987, its behavior can be interpreted by assuming two four-wave mixing (FWM) regions, as MacDonald and Feinberg did for the ''cat'' quantum superposition of state conjugator [2]: each of the two incident beams interacts with the beam fanning (BF) [3] it generates, creating the index grating necessary for FWM to build up. It is thus the double diffraction on two successive FWM gratings that generates the phase conjugate waves.

However, the stabilization of the conjugate waves is one of the main difficulties of its practical implementation. Itoh *et al.* [4] have, for instance, reduced the instabilities in a cat conjugator by aligning the incident beam to the Brewster angle, thus ensuring minimum internal reflections of the conjugated beam. This can be done for both DPCM beams, but does not reduce the DPCM oscillating behavior as well as for the cat conjugator.

Indeed, if we interpret the oscillations observed as a competition between BF and the DPCM it has generated, aligning to the Brewster angle is not the appropriate solution, though it helps by eliminating unwanted reflections. We thus aim at suppressing the competition by making BF and DPCM work with the same photorefractive gratings. This can be realized if both incident beams share the same fanning direction (Kamshilin *et al.* have successfully performed experiments of this kind in $Bi_{12}TiO_{20}$ [5]), the gratings responsible for BF being then the same as those used for FWM. We believe that this situation would increase both efficiency and stability of the $BaTiO_3$ DPCM, and at the same time decrease the characteristic time of the process.

Since DPCM stems from the common fanning of both incoming beams [6], if both could be set so as to generate *most of the* fanning in the same direction, though counterpropagating, DPCM would hopefully establish itself along that common direction, thus drastically reducing the need to compete with BF. Figure 1 shows such a case, with the DPCM establishing in the common fanning direction of both incident beams.

In the following, we will recall and briefly describe a model for beam fanning—based on the two-wave mixing interpretation of the phenomenon [7], which allows the determination of the best possible angles of incidence for the beams [8]. As this model predicts drastically different behaviors for *narrow* and *broad* beams, the frontier between them is detailed in [8] and will be recalled further on, the corresponding DPCM optimization method will equally vary if

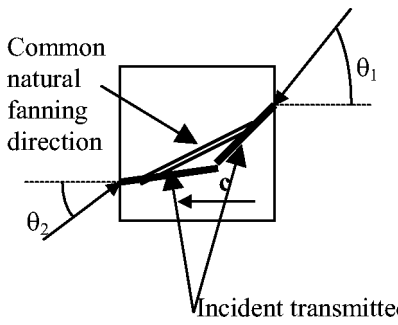

FIG. 1. Double phase-conjugate mirror configuration using a common fanning direction of both incident beams.

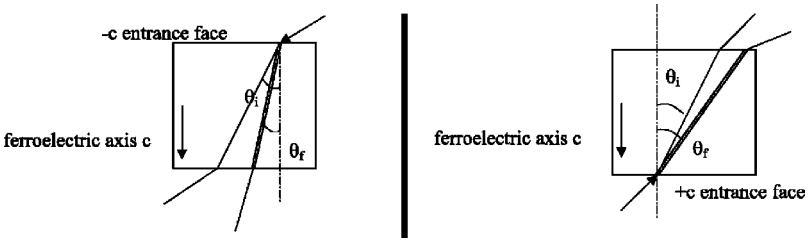

FIG. 2. Definition of the $+c$ and $-c$ entrance faces of the crystal.

narrow or *broad* beams are used.

Thus, starting with the definition of the experimental setup, we will review the BF model and apply it to experimental DPCM optimization, starting with *narrow* beams and generalizing to *broad* beams. Finally, the technique and the BF/DPCM models and interpretations it relies on will be tested further by analyzing the optimization technique to be applied to a DPCM that allows one *narrow* and one *broad* beam to interact.

II. EXPERIMENTAL SETUP

Two photorefractive $BaTiO_3$ samples have been used for DPCM optimization: a nominally undoped $BaTiO_3$ ($4.38\ \text{mm}\times 3.02\ \text{mm}\times 4.39\ \text{mm}\|\vec{c}$) which was grown in the Chinese Academy of Sciences of Beijing and a $BaTiO_3$:Co (called doped crystal) with 20 ppm in the melt ($5\ \text{mm}\times 2.6\ \text{mm}\times 5\ \text{mm}\|\vec{c}$) grown at FEE [14]. The source is an Ar^+ ion laser ($\lambda = 514$ nm) with a maximum output power of 75 mW and a $1/e^2$ Gaussian beam waist of 0.5 mm. Prior to reaching the sample, the beam goes through an optical isolator in order to prevent the laser from being perturbed by conjugated waves. The light entering the crystal has an extraordinary polarization by means of a rotating half wave plate and enters the sample through the faces that are orthogonal to the ferroelectric axis $\vec{c}$. The original beam is split into two beams, and a shutter is placed in each arm to control the beginning of the experiment. Each beam is focused on a horizontal plane at the entrance of the crystal by means of a cylindrical lens in order to avoid conical diffraction [9,10]. The beam waist in the orthogonal direction on the entrance face of the crystal is controlled by means of a second cylindrical lens, its axis being perpendicular to that of the first one. The sample lies on automated rotation and translation stages in order to accurately control the lateral position and the angle of incidence of the beam (with a precision of 1 μm and 1/1000°).

We have to point out that the beams have been focused on the entrance face of the crystal. The region in which they can be assimilated to plane waves (the Rayleigh region), necessary for the approximation used later has to be longer than the crystal. With the parameters used in our experiment, the smallest possible length of the Rayleigh region is 4.8 mm for a crystal with an index of $n = 2.4$. In this case, we can neglect the diffraction of the beams inside the crystal and consider the $1/e^2$ width as constant.

III. PRELIMINARY DEFINITIONS

Let us name $-c$ face the entrance face for a beam entering the crystal in the direction of the ferroelectric axis and $+c$ face the opposite one (see Fig. 2). For notation convenience, we use index 1 for values relative to the $-c$ face, and index 2 to the ones relative to the $+c$ entrance face.

As stated before [8], in order to predict the direction carrying most of the fanned intensity—which we will call the *fanning direction*—we consider the model of beam fanning, in which the incident beam performs two-wave mixing (TWM) with light scattered in all directions by the inhomogeneities of the crystal [7,11,12]. The fanning direction is the one which is mostly amplified by this process. Starting from that hypothesis, we will theoretically determine the fanning direction that is associated to any given incoming direction. We will show that this direction corresponds to the experimentally measured direction of the maximum of intensity in the fanning patterns which we obtain. We have to point out here that in those patterns which are shown in Ref. [8], the width of the incident beams is very small as compared to what can be found elsewhere in the literature. This enables us to identify clearly a fanning direction as specified before.

The incoming and fanning directions will be referred to as oriented angles with respect to the ferroelectric axis $\vec{c}$, both for the experimental and the theoretical approaches:

(1) θ_i stands for the angle *inside* the crystal between the direction of the ferroelectric axis and the linearly transmitted beam—which we call incident beam in the following.

(2) θ_f stands for the fanning angle, *i.e.*, the angle *inside* the crystal between the direction of the ferroelectric axis and the fanning direction as defined above.

These angle notations are summarized in Fig. 2.

The analysis that will be conducted in the following is also based on beam width. Let us precise here that the beam width that will be taken into account is the $1/e^2$ beam width taken perpendicularly to the propagation direction. Furthermore, the beam width we will refer to are taken *outside* the crystal, before refraction takes place.

Finally, let us precisely recall the distinction made in Ref. [8] between *narrow* beams and *broad* beams: as shown in Fig. 3, a beam is called *narrow* if it overlaps completely with its fanned beam within the sample. (We consider here the $1/e^2$ width of the beam as defined before, that is to say that a slight part of the light is not taken into account.) It is otherwise called *broad*. It is important to note that, under this definition, one beam of a given $1/e^2$ width can be considered either *broad* or *narrow* depending on its incident angle.

IV. NARROW BEAM DPCM

A. Predicting the fanning direction

We use here the well-established theory (Ref. [7] and references therein) according to which BF is due to photorefrac-

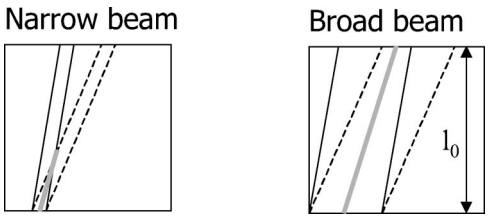

FIG. 3. Definition of *narrow* and *broad* beams. The incident beam goes towards the top of the crystal.

tive amplification through TWM of seed light diffused on the inhomogeneities of the crystal entrance face. In the case of narrow beams, for two samples of $BaTiO_3$ (undoped and 20 ppm Co doped) and for the two incident faces presented in Figure 2, we have therefore determined the fanning direction as a function of the incident angle by deriving the photorefractive gain with respect to the fanning direction angle θ_f. The expression of the photorefractive gain as a function of both incident and amplified—fanning—direction has been given by Cronin-Golomb *et al.* [13]. This leads us to a relationship linking θ_i and θ_f which has been numerically evaluated [8].

Using one fit parameter proportional to the trap density, leading to one unique fit per sample, we have determined theoretical curves corresponding to both entrance faces, and checked it against experimental results. Figure 4 shows the resulting theoretical predictions against the experimental measures for both the samples included in this study and for both faces, which we presented in a former paper [8].

B. Optimizing the DPCM

It is now possible to use the lower theoretical curve in Fig. 4 to determine the corresponding fanning angle for any incident angle on entrance face $-c$. The curve corresponding to face $+c$ will allow us to determine the incident angle corresponding to this fanning direction, which will then be shared by both incident beams.

As pointed before [4], reflection of the conjugate waves at the output face of the crystal is one other reason that makes DPCM unstable. The choice of incident angles as near as possible to the Brewster angle can help avoiding this difficulty. In $BaTiO_3$, the value of the refraction index is $n=2.4$. Therefore, in the crystal, the Brewster angle is equal to $\theta_B=22.6°$. For values of the incident angles below θ_B, the reflection coefficient is less than 20%. For angles above this value, it grows strongly. With both incident angles equal to the Brewster angle, the model which we developed for fanning shows that it is impossible to get both beams to have the same fanning direction. To have a good compromise, we have decided to choose the highest incident angle θ_i^1 equal to the Brewster angle, that is in $BaTiO_3$: $\theta_i^1=22.6°$.

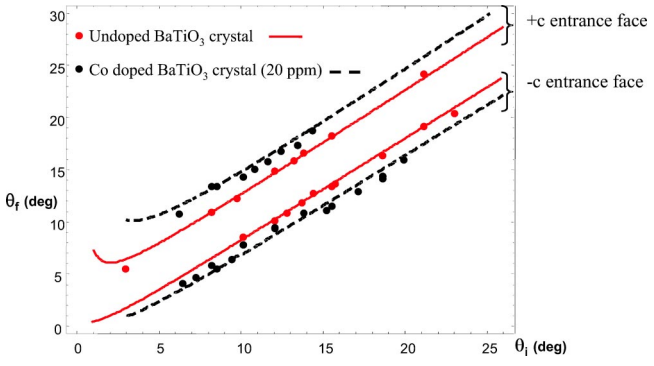

FIG. 4. Fanning angle measured and calculated as a function of the incident angle in two different crystals and for two different entrance faces in the case of a narrow incident beam.

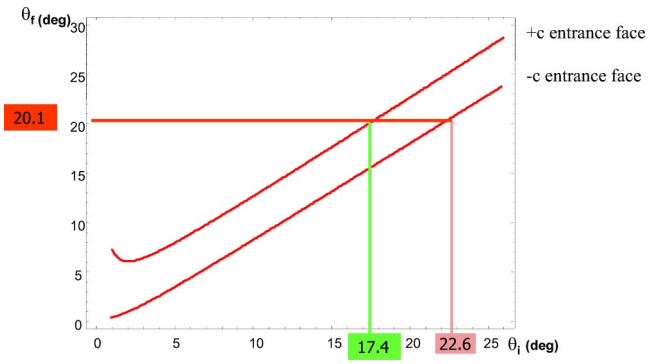

FIG. 5. Example of incident angles determination by using the theoretical curves for fanning relative to the considered crystal.

The theoretical determination is shown in this practical case in the undoped sample in Fig. 5. The value chosen for θ_i^1 dictates the choice for $\theta_i^2=17.4°$. Under these angular conditions, assuming narrow beams (the waists are $w_0^1=25$ μm and $w_0^2=45$ μm) and equal incident powers, $P_1=P_2=100$ μW, the optimum overlapping of the fanning has been searched, the common fanning direction being along $\theta_f=20.1°$.

Under the formerly described conditions, we have obtained double phase conjugation reflectivity presented in Fig. 6 in the undoped crystal. The measured reflectivities reached 35% for one incident beam and 32% for the other one and a very good stability (about 3% for a 3 h measurement). These values are considered inside the crystal taking the Fresnel reflection into account. The phase-conjugate waves build up with the same dynamics as beam fanning. Therefore, we fitted the rising period to a characteristic temporal evolution of photorefractive phenomena, and we found that the response time is less than 1 s. Decreasing the incident power down to 10 μW, we still obtained phase conjugation with stable reflectivities of 33% and 30% and a response time of 11 s.

The same process has been applied to the doped sample, the results are shown in Fig. 7. Here again $\theta_i^1=22.6°$, which leads to a value of the second incident angle $\theta_i^2=14.1°$. The incident powers were taken equal to $P_1=P_2=200$ μW. We can see that the conjugate waves show once again a very good stability . They exhibit not very high reflectivities of 13% and 10% in this case as compared to the undoped crystal. One explanation for these results is that the crystal has been doped and designed for a longer wavelength of the incident beams. The photorefractive gains corresponding to the various couples of angles to be considered here are in accordance with the observations. Moreover, the absorption

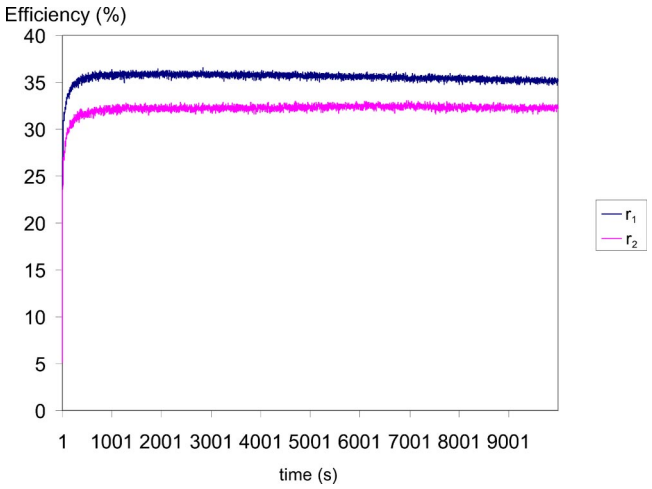

FIG. 6. Evolution of the reflectivities measured in each arm of the setup. Best results obtained in the undoped crystal in terms of efficiency and stability.

(higher in the doped crystal) prevents a part of the incident beams from taking part to DPCM.

C. Testing the model

In order to validate the idea that it is the overlapping of predicted fanned beams that allows good stability, fast response, and high reflectivity, we have studied the influence of spatial shifts on each beam. The effects of the translation of one beam in both transversal and vertical directions have been investigated by performing micrometric translation in each direction. The results obtained in terms of efficiency of the conjugation as a function of the distance between the fanned beams are shown in Fig. 8 in the case of the translation in the plane comprising incident beam, fanned beam and $\vec{c}$ axis, and in Fig. 9 for the orthogonal one which means with vertical shift. Both figures are made in the case of the undoped crystal. The same behavior was observed in the doped one. In each case, we were able to find an optimum of reflectivity that is simultaneously attained for both conjugated beams. We observed that the maximum of reflectivity corresponds to the position which gives the best stability. The behavior of the conjugate beams corresponding to translations in the plane comprising the incident and fanned beams is not symmetric (Fig. 8), whereas the one corresponding to the orthogonal plane is symmetric (Fig. 9). This can be explained by the influence of the beam fanning experienced by the incident beams. Beam fanning ''attracts'' any incident beam in the direction of the ferroelectric axis. For our experiments, the axis is in a horizontal plane, therefore it is equivalent to perform either up or down vertical displacement. On the contrary, a lateral displacement of a beam which is not colinear to the axis gives nonsymmetric results. Such displacement can, for example, give birth to self-pumped phase conjugation of the part of the fanned beam which is no more in the influence of the contrapropagating one, by the use of reflections on the internal faces of the crystal. The curves obtained in Figs. 8 and 9 are also different in the acceptable distance between the fanning beams that allow DPCM to establish. Namely, in the case of lateral shift, the beams can be distant from ± 150 μm without a noticeable deterioration of the signal (90% of the maximum), whereas the equivalent authorized vertical shift is

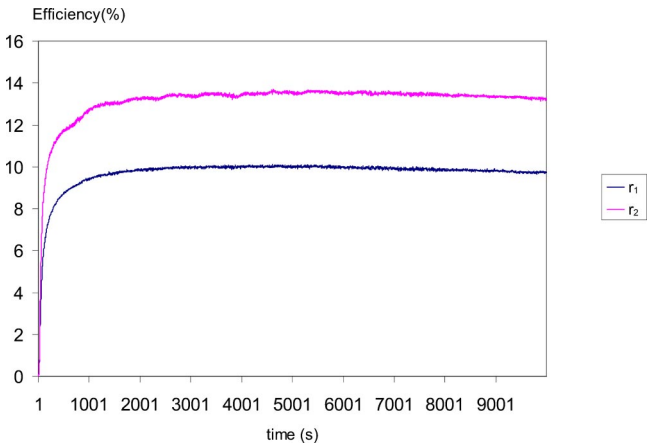

FIG. 7. Evolution of the reflectivities measured in each arm of the setup. Best results obtained in the doped crystal in terms of efficiency and stability.

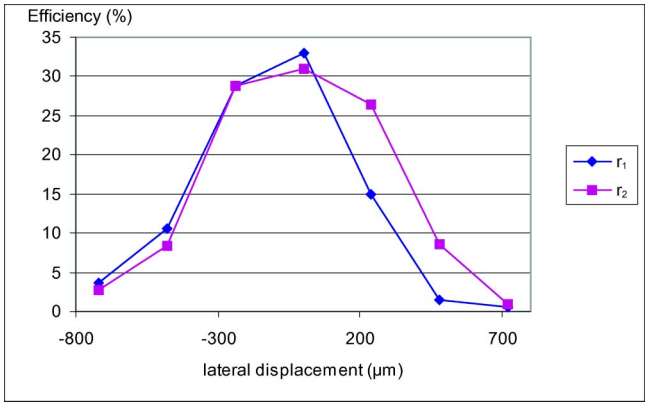

FIG. 8. Evolution of the steady-state efficiency of DPCM versus lateral displacement of one beam in the plane comprising both the incident and fanned beams.

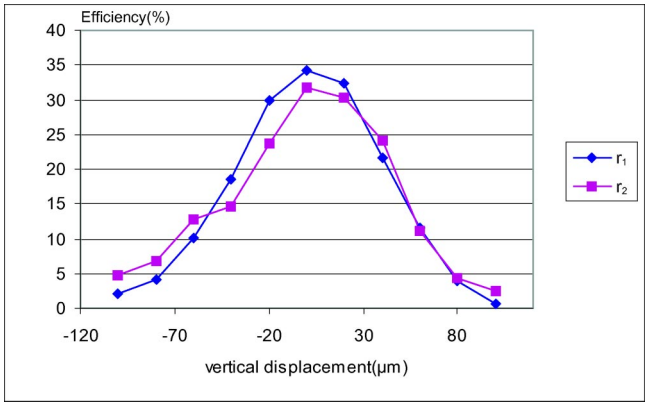

FIG. 9. Evolution of the steady-state efficiency of DPCM versus lateral displacement of one beam in the plane orthogonal to that comprising both the incident and fanned beams.

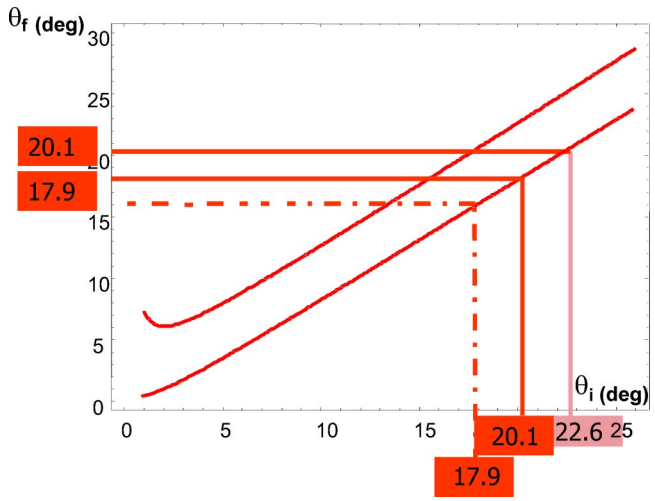

FIG. 10. Determination of the fanning angle for a broad incident beam. Cascaded use of the theoretical curves obtained before.

around ± 30 μm. This is due to both the respective dimensions of the fanned beams in both directions (for both beams: 100 μm in the horizontal plane and 33 μm in the orthogonal direction) and the influence of the axis that can make beams in the same plane conjugate even if they overlap very slightly. Let us finally point out that the above given beam widths are actually the $1/e^2$ widths, which means that beams which are not formally overlapping do actually overlap a little, and can thus generate some beam conjugation. We noted that the rising time of the conjugate waves is the smallest in the case of maximum overlapping, and in this case the reflectivity is also the best observed.

V. BROAD BEAM DPCM

Keeping the same incident angles as defined before for the undoped crystal, we have tried to enlarge both incident beams. It appears that once the threshold between *narrow* and *broad* beams is exceeded, the previously reached stability and efficiency of the phase-conjugate reflectivity vanish.

This can be explained through the BF model that we have developed previously [8]: when beams are *broad* the fanning direction has to be determined, through the use of the theoretical curves as it is presented in Fig. 10, by iterating the process until the incident beam can be considered as *narrow*; if a given incident beam generates fanning in another given direction, this new beam can, if the incoming beam is *broad*, be considered as a new incoming beam and itself generate fanning in yet another direction, that we will call the next *order*. This process stops only when the fanned beam eventually becomes *narrow* by the fact that its direction angle grows at each step.

This iterative multiorder process is summarized in Fig. 10 for waists $w_0^1=49$ μm and $w_0^2=98$ μm: the fanning direction of the incoming beam 1 would have been 20.1° if it had been *narrow*, but this latter fanned beam has to be considered as a new incoming beam—*narrow*, this time—which will amplify another fanning direction at the angle of 17.9°. The process stops since the 20.1° beam is *narrow*.

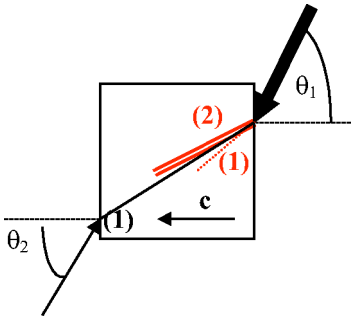

FIG. 11. Experimental conditions chosen for an intermediate fanning angle. Dashed line stands for the first-order fanning direction, double line for the second order. The black line represents the shared fanning direction which enables DPCM to work.

Let us point out one important thing: The fanning patterns which can be found in the literature do not correspond to ours. This is due to the fact that most of these studies have been carried out with beams several orders of magnitude *broader* than the smallest *broad* beam in the sense that is defined here. This yields a large number of orders of fanning and, though the maximum intensity is still carried out by the last order, the small remaining intensity carried by each previous orders makes the experimentalist see a continuous fanning pattern.

VI. FURTHER EVIDENCE: MIXED BEAM DPCM

In order to give a more complete demonstration of the validity of the hypothesis given above and subsequently of the optimization process for DPCM, we have performed further experiments aiming to prove the existence of a *main* direction of fanning on one hand, and of the iterating process that allows to predict the fanning of broad beams on the other hand. For that, we have chosen a broad incident beam on face 1, giving fanning in the second order direction as defined above. The incident angle is still $\theta_i^1=22.6°$. Two different cases of double phase conjugation have then been tested, namely, DPCM building by way of a fanning direction situated between the first and second order, and DPCM using a second-order fanning direction. Both cases are presented hereafter.

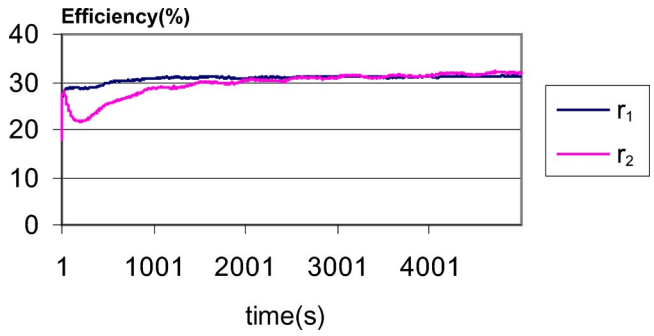

FIG. 12. Best results obtained in terms of efficiency with an intermediate fanning angle.

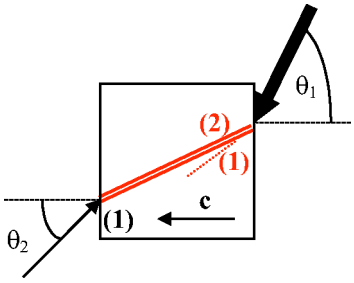

FIG. 13. Experimental conditions chosen for a fanning angle of the narrow beam corresponding to the second-order fanning direction of the broad beam. Dashed line stands for the first-order fanning direction, double line for the second order which is the shared fanning direction which enables DPCM to work.

A. DPCM uses an intermediate fanning direction

We have tried to obtain double phase conjugation with beam 2 chosen narrow and with its unique fanning direction between the first ($\theta_f = 20.1°$) and second ($\theta_f = 17.9°$) order for beam 1 (Fig. 11). In this configuration, we have searched for the best overlapping of the beams by translating one of them in the plane comprising both incident and fanned beams and the other orthogonally. The optimization of both the efficiency and the stability of the DPCM lead to the results shown in Fig. 12.

The oscillation at the start of the process can be interpreted as DPCM occurring successively on the first or the second order of fanning, finally choosing the second. This can be inferred from the dynamics of the iterating process of fanning, whose details can be found in Ref. [8]: the first order appears first, prior to eventually decreasing, yielding its energy to the second order.

B. DPCM uses a second-order fanning direction

We have then chosen $\theta_i^2 = 15.1°$ so that the main fanning of this narrow beam is strictly superposed to the second-order direction of fanning of beam 1: $\theta_f = 17.9°$ (Fig. 13). Under these conditions we have managed to obtain both stable and efficient DPCM. The best results are presented in Fig. 14, thus confirming the need to consider the iterating process for *broad* beams and establishing the use of considering the *fanning direction*, i.e., the main direction of fanning, instead of dealing with the whole fanning pattern.

We can point out that the best efficiency obtained is smaller than in the case of two narrow beams. We can justify this by considering the photorefractive gain (directly linked to the efficiency) obtained in the different situations tested. For beam 1, the first-order fanning direction is indeed nearer to the incident beam than the second order. This explains

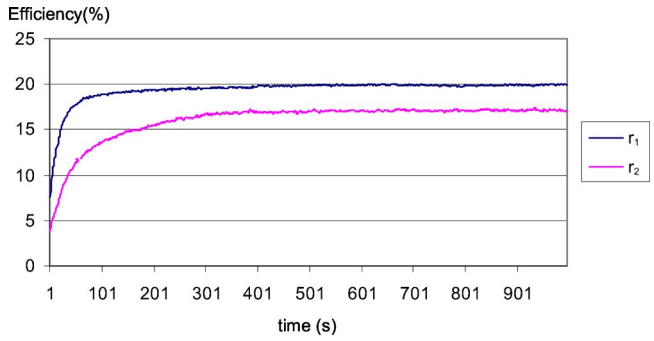

FIG. 14. Results obtained with a second-order fanning direction.

why the photorefractive gain and therefore the efficiency of FWM for beam 1 is higher in the first case than in the second. For beam 2, the angular distance between incident and fanned beam happens to be 1.7° for two narrow beams and 2.8° for DPCM using the second fanning direction. Both the gratings that participate in the DPCM process thus exhibit higher gains when two narrow beams are present: this explains the higher reflectivities for narrow beams.

VII. CONCLUSION

We have used a formerly described model [8] for beam fanning in order to choose the conditions of various DPCM experiments. The results obtained in terms of efficiency and stability are in total agreement with our predictions. In the case of narrow beams, we have obtained the best results for two incident beams sharing the same fanning direction. Moreover, we have managed to obtain stable though less efficient DPCM with one broad and one narrow incident beams sharing the same fanning direction. All other cases tested have led to unstable phase conjugation. It can also be noticed that the optimum configuration for one crystal is valid in terms of efficiency as well as stability or response time.

We believe that further investigations would be of interest. In particular, we suggest the use of specially cut crystals, for which the incident faces would allow to have the highest possible photorefractive gain inside the crystal together with the Brewster angle on each incident side.

ACKNOWLEDGMENTS

The authors would like to thank Dr. D. Rytz, from the Forschunginstitut für mineralische und metallische Werkstoffe Edelsteine/Edelmetalle (Idar-Oberstein, Germany) for his $BaTiO_3$:Co crystal on which part of our experiments were conducted. This work was supported in part by the Région Lorraine.

[1] S. Weiss, S. Sternklar, and B. Fischer, Opt. Lett. **12**, 114 (1987).
[2] K.R. MacDonald and J. Feinberg, J. Opt. Soc. Am. **73**, 548 (1983).
[3] J. Feinberg, J. Opt. Soc. Am. **72**, 46 (1982).
[4] S. Itoh, Y. Uesu, N. Oh-hori, and S. Odoulov, Appl. Phys. B: Lasers Opt. **B68**, 953 (1999).
[5] A.A. Kamshilin, V.V. Prokoviev, and T. Jaaskelainen, IEEE J.

Quantum Electron. **31**, 1642 (1995).
[6] A.M.C. Smout, R.W. Eason, and M.C. Gower, Opt. Commun. **59**, 77 (1986).
[7] M. Segev, D. Engin, A. Yariv, and G.C. Valley, Opt. Lett. **18**, 956 (1993).
[8] C. Mailhan, M. Goetz, N. Fressengeas, and G. Kugel, J. Soc. Am. B **18**, 64 (2001).
[9] N. Wolffer, Ph. Gravey, and V. Roger, Opt. Commun. **89**, 380 (1992).
[10] Q.B. He, P. Yeh, C. Gu, and R.R. Neurgaonkar, J. Opt. Soc. Am. **9**, 114 (1992).
[11] M. Segev, Y. Ophir, and B. Fischer, Opt. Commun. **77**, 265 (1990).
[12] Y.H. Hong, P. Xie, J.H. Dai, Y. Zhu, H.G. Yang, and H.J. Zhang, Opt. Lett. **18**, 772 (1993).
[13] M. Cronin-Golomb, B. Fisher, J.O. White, and A. Yariv, IEEE J. Quantum Electron. **20**, 12 (1984).
[14] Forschungsinstitut für mineralische und metallische Werkstoffe Edelsteine/Edelmetalle GmBH, Idar Oberstein, Germany.